Conformational Changes of a Surface-Tethered Polymer during Radical Growth Probed with Second-Harmonic Generation

Deckers, Steven; Bloemen, Maarten; Koeckelberghs, Guy; Glorieux, Christ; Verbiest, Thierry; Van der Veen, Monique A.

DOI
10.1021/acs.langmuir.7b00172

Publication date
2017

Document Version
Final published version

Published in
Langmuir: the ACS journal of surfaces and colloids

LANGMUIR

Article

pubs.acs.org/Langmuir

Conformational Changes of a Surface-Tethered Polymer during Radical Growth Probed with Second-Harmonic Generation

Steven Deckers,*[,†] Maarten Bloemen,[†] Guy Koeckelberghs,[†] Christ Glorieux,[‡] Thierry Verbiest,[†] and Monique A. van der Veen*[,§]

[†]Department of Chemistry, University of Leuven, 3001 Leuven, Belgium

[‡]Laboratorium voor Akoestiek en Thermische Fysica, Departement Natuurkunde en Sterrenkunde, Katholieke Universiteit (KU) Leuven, Celestijnenlaan 200D, 3001 Heverlee, Belgium

[§]Catalysis Engineering, Applied Sciences, Delft University of Technology, 2629 Delft, Netherlands

Supporting Information

ABSTRACT: The surface-induced polymerization of a chromophore-functionalized monomer was probed *in situ* for the first time using a nonlinear optical technique, second-harmonic generation. During the first hours of the polymerization reaction, dramatic changes in the tilt angle of the chromophore-functionalized side groups were observed. Following evaluation of the nonlinear optical data with those obtained from atomic force microscopy and ultraviolet−visible, we conclude that second-harmonic generation efficiently probes the polymerization reaction and the conformational changes of the surface-grafted polymer. With polymerization time, the conformation of the surface-tethered polymer changes from a conformation with the polymer backbone and its side groups flat on the surface, i.e., a "pancake" conformation, to a conformation where the polymer backbone is stretched away combined with tilted side groups or an enlarged tilt angle distribution, i.e., a "brush-type" conformation.

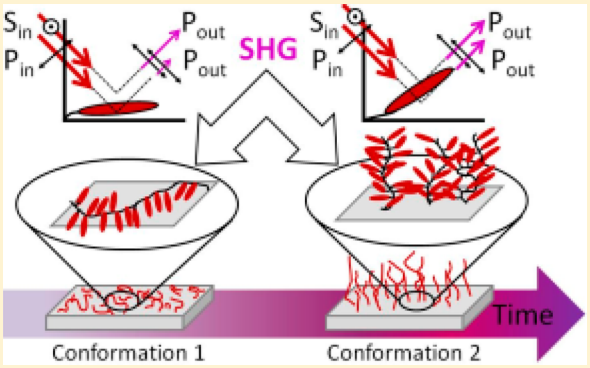

INTRODUCTION

Surface-initiated activators regenerated by electron transfer atom transfer radical polymerization (SI-ARGET ATRP)[1] is based on one of the most versatile and, consequently, intensely used radical polymerization techniques.[1−4] The technique combines ATRP with an excess of reducing agent, to provide a method for grafting polymers from substrates with a reduced oxygen sensitivity.[1,5] However, characterization of the surface-grafted polymers on low specific area substrates is challenging. The small amount of resulting polymeric material, covalently attached to the surface, rules out commonly used characterization techniques, such as methods based on size-exclusion chromatography.[6−8] Instead, techniques such as atomic force microscopy (AFM), ellipsometry, X-ray photoelectron spectroscopy (XPS), and near edge X-ray absorption fine structure (NEXAFS) are often used.[7,9] These techniques have been used with wetted or dried samples, generally *ex situ* with respect to the polymerization reaction. Apart from AFM, they do not offer direct information on the polymer conformation, and in addition, as a result of the nature of the characterization technique itself or the strong impact of the post-synthetic treatment of the surface-tethered polymers, an altered polymer layer thickness is obtained.[10,11] In view of that, we have employed a second-order nonlinear optical (NLO) technique, second-harmonic generation (SHG), to study the polymer growth and conformation changes during the different stages of the SI-ARGET ATRP reaction, *in situ* and *ex situ* with respect to the polymerization reaction. SHG is inherently surface-specific and can be used to determine the possible distribution widths of an average molecular tilt angle.[12−14] Moreover, SHG can be used to follow dynamical processes at interfaces *in situ*.[15,16] As a result of these strengths, a few reports already exist on the use of second-order NLO methods to characterize SI-ATRP-grafted polymers,[17−19] although in all of these works, the polymers were grown *ex situ*.[17−21] The first NLO measurement on a polymer brush synthesized by ATRP was SHG from a chromophore-functionalized polymer grafted from a macroinitiator.[19] The resulting polymer had to be poled with an electrical field to induce a second-harmonic signal. Second-harmonic light scattering (SHS) has also been used to study the dynamics of the hydrodynamic thickness of polymer brushes grafted from suspended nanoparticles and the dependence upon the ionic strength of the solution.[18] Sum frequency generation (SFG) has been used to study the dependence of the thickness of a polymer brush upon the solvent pH and concentration and nature of dissolved ions.[17]

Received: January 17, 2017
Revised: March 24, 2017
Published: April 12, 2017

DOI: 10.1021/acs.langmuir.7b00172
Langmuir 2017, 33, 4157−4163

In this work, we present the first *in situ* second-order NLO study of the growth of a grafted polymer brush. This allowed us to probe the conformation during polymerization: with increasing synthesis time, the polymer side chains become more perpendicularly oriented with respect to the substrate. We confirmed the same trend for the *ex situ* grafted polymer. After comparison to data from ultraviolet−visible (UV−vis) and AFM, we conclude that SHG efficiently probes both the thickness increase and conformation change at the same time.

EXPERIMENTAL SECTION

Two samples consisting of a SI-ARGET ATRP-grafted poly((*E*)-6-(ethyl(4-((4-notrophenyl)diazenyl))phenyl)amino)hexyl methacrylate) were used. Both samples were synthesized using the same synthetic procedure, as schematically depicted in Scheme 1.

Scheme 1. Scheme of the Synthetic Procedure of the SI-ARGET ATRP-Grafted Polymers

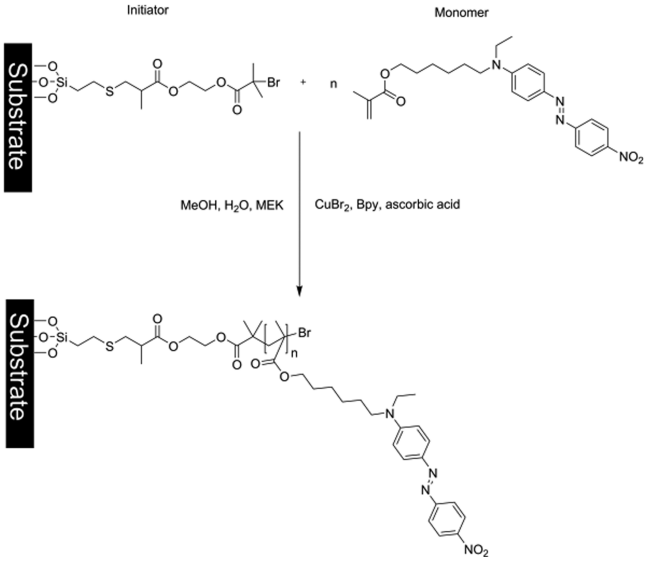

In the remainder of the text, poly(DR1-hexyl methacrylate) will be used to refer to the synthesized polymer. The *ex situ* sample was synthesized prior to the SHG measurement in a separate vial, while the *in situ* sample was grafted *in situ* during SHG measurements. The SHG measurements were performed using an 800 nm wavelength, femtosecond (fs)-pulsed laser setup, with the laser beam used in reflection geometry at an angle of 45° (θ) with respect to the sample normal (see Figure 1). This angle should not be confused with the

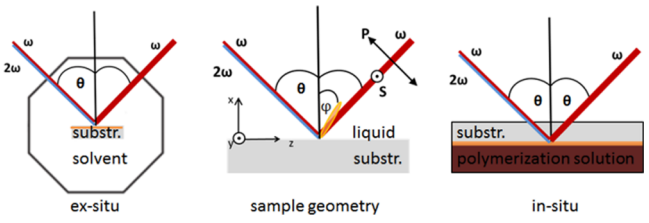

Figure 1. (Middle) Experimental configuration of the measurement setup and the coordinate system used to define the NLO tensor components, (left) configuration of the SHG measurements of the *ex situ* sample, which is in contact with a clear solvent mixture, and (right) configuration of the SHG measurements of the *in situ* sample, which is in contact with the strongly light-absorbing polymerization solution. The orange line is used to denote the polymer layer, while "substr." is used to denote the substrate.

average molecular tilt angle φ of an adsorbed molecule (orange ellipse in Figure 1) to the surface normal. The measurement setup comprises a collection of lenses, filters, polarizing and analyzing optics, positioned before and after the sample, to enable the measurement of P-polarized SHG light using incident laser light with a variable polarization direction. The two ultimate polarization directions of the incident laser light (with optical frequency ω), P and S polarization, are schematically shown in the middle image of Figure 1. During the SHG measurements, both samples are in contact with a liquid. The liquid consisted of a mixture of methanol/water/methyl ethyl ketone in the case of the *ex situ* sample (left image in Figure 1) and the polymerization solution in the case of the *in situ* sample (right image in Figure 1). Because the polymerization mixture contained the strongly absorbing monomers as well as highly colored metal complexes,[22−24] the SHG light (2ω) is prevented to propagate through the absorbing liquid by measuring from the opposite side of the surface (see Figure 1). In other words, with the *in situ* sample, the measurement is performed through the substrate, while the *ex situ* measurements are performed through the liquid. To limit side effects by laser-induced heating of the polymerization solution while maximizing the amount of experimental data, the SHG measurements on the *in situ* sample are divided between three positions on the substrate (see the Supporting Information). Although interactions of the charged complexes as used in the polymerization protocol on the surface NLO effect have been reported in recent literature, they were neglected in this study because we used a NLO-optimized chromophore.[25−27]

Details of the general synthesis procedure and further experimental details of the additional optical and thickness measurements can be found in the Supporting Information.

RESULTS AND DISCUSSION

The synthesized polymer consists solely of chromophore-modified methacrylate monomers. The chromophores are located in the side groups of the monomer and are linked to the polymeric backbone by a hexyl linker group. Both samples consist of these polymers that are grafted from initiator-coated glass substrates. The SHG signal intensity is caused by the chromophore side groups and is proportional to the square of the total NLO susceptibility.[28−30] As seen in eq 1, in the case of adsorbates, the latter equals the sum of three contributions, one from the substrate, one from the chromophores, and one from the interaction between both[28]

$$\chi^{(2)} = \chi^{(2)}_{\text{substrate}} + (\chi^{(2)}_{\text{interaction}}(t) + \chi^{(2)}_{\text{polymer}}(t)) \quad (1)$$

with the latter contributions being time-dependent. More specifically, $\chi^{(2)}_{\text{polymer}}$ is dependent upon the length and conformation of the grafted polymer chains. No SHG signal was observed from the bare and initiator-modified surface. Hence, contributions from the substrate and the interaction of the substrate with the chromophores to the NLO signal can be neglected. The NLO signal is dominated by the chromophores on the side chains. Both series of samples are treated as in-plane isotropic collections of chromophores, because the chromophore side groups have no preferential orientation, apart from the orientation arising from their linkage to the polymer backbone.[31−34] In the case of our polymer system, the NLO behavior is controlled by a single tensor component β_{zzz}, aligned with the conjugation path along the long axis of the chromophoric group of the monomer.[34,35] To obtain information about the conformation of the chromophoric side groups, polarization-dependent SHG data were taken by rotating the polarization direction of the incident laser light, while the P-polarized SHG light was detected. The polarization direction of the laser light was altered using a half-wave plate (HWP, Thorlabs WPH05M-808). The resulting SHG data

DOI: 10.1021/acs.langmuir.7b00172
Langmuir 2017, 33, 4157−4163

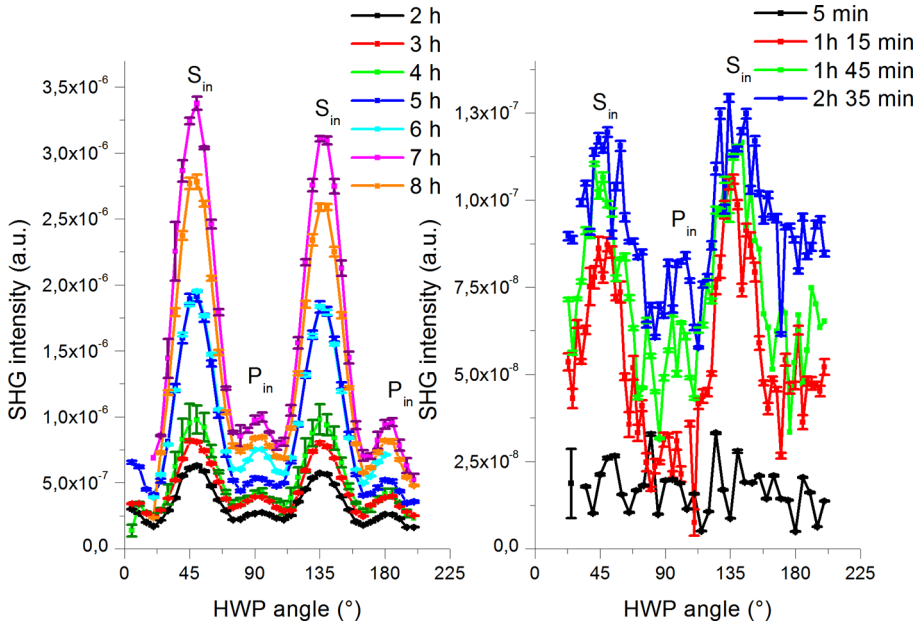

Figure 2. Polarized SHG data of the (left) *ex situ* grafted sample and (right) *in situ* grafted sample. The P-polarized light, the light polarized parallel with the plane of incidence, is situated at HWP angles at even multiples of 45°, while the S-polarized light, which is polarized perpendicularly to the plane of incidence, is situated at uneven multiples of 45°. S_{in} and P_{in} denote the polarization direction of the incident laser light.

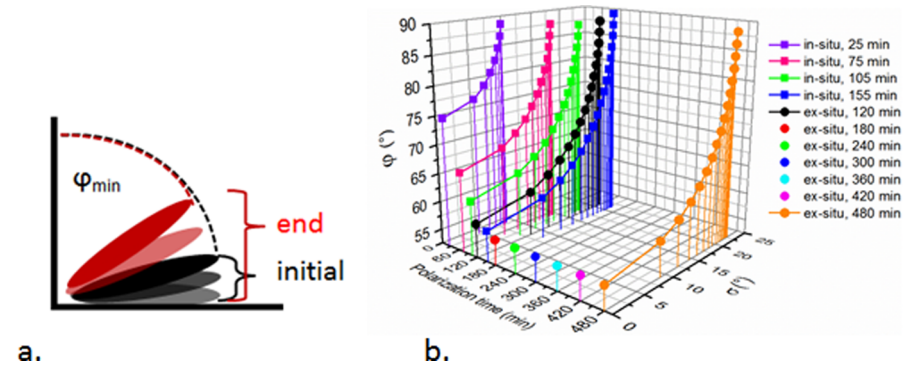

Figure 3. (a, Left) Cartoon illustrating the possible apparent tilt angles of the chromophoric side groups of the polymer in the initial (represented by the initial distribution of the *in situ* grafted sample, black) and final (represented by the distribution of the *ex situ* grafted sample, red) stages of the polymerization, determined by polarization-dependent SHG. (b, Right) Possible combinations of root-mean-square distribution widths σ and average tilt angles for selected SHG measurements.

were corrected for fluctuations in laser stability[36] (see the Supporting Information). The polarization-dependent SHG data obtained from the *in situ* and *ex situ* grafted sample at various polymerization times are plotted as a function of the polarization angle of the incident laser light in Figure 2. Data points at even multiples of 45° represent the SHG signal from P-polarized incident light, while data points at uneven multiples of 45° represent the SHG signal from S-polarized incident light. In Figure 2, P_{in} and S_{in} is used to denote the polarization direction of the incident light. The error bars that represent the measurement error of the data point (as is the case with most samples) are drawn in the same color as the data point, while the error bars that represent the measurement error of different measurements, with the sample rotated 180° with respect to the surface normal (as is the case with the 4 and 7 h *ex situ* samples), are drawn in a darker color (see the Supporting Information). In case of the *in situ* sample, data from only one of the three probed positions is shown in Figure 2 (the rest can be found in the Supporting Information). For both the *in situ* and *ex situ* grown samples, the largest SHG intensity is found for incident light polarized in the S direction (see Figure 1), while a smaller maximum emerged in the case of P-polarized laser light. In addition to the global signal intensity increase with polymerization time, which confirms that the NLO signal is arising from the monomers added to the grafted polymer chain, the background NLO signal also rises. We were able to fit the data using a $C_{\infty v}$ model (neglecting any contributions from scattering that would be largely polarization-independent); hence, we conclude that any contributions to the NLO signal resulting from scattering are insignificant. An exception to the systematic signal intensity increase occurs for the *ex situ* sample, between 7 and 8 h of polymerization time. The exception can be caused by different processes. First a divergence of the rate of the polymerization reaction can occur at high polymerization times; i.e., the controlled nature is lost. This is commonly present in the final stages of a SI-ATRP reaction and results in an increased conformational freedom (or decreased anisotropy) of the resulting polymer.[37] A second explanation, which is in agreement with our UV−vis spectra (see Figure 4), is that the sample taken at 8 h contains less

DOI: 10.1021/acs.langmuir.7b00172
Langmuir 2017, 33, 4157−4163

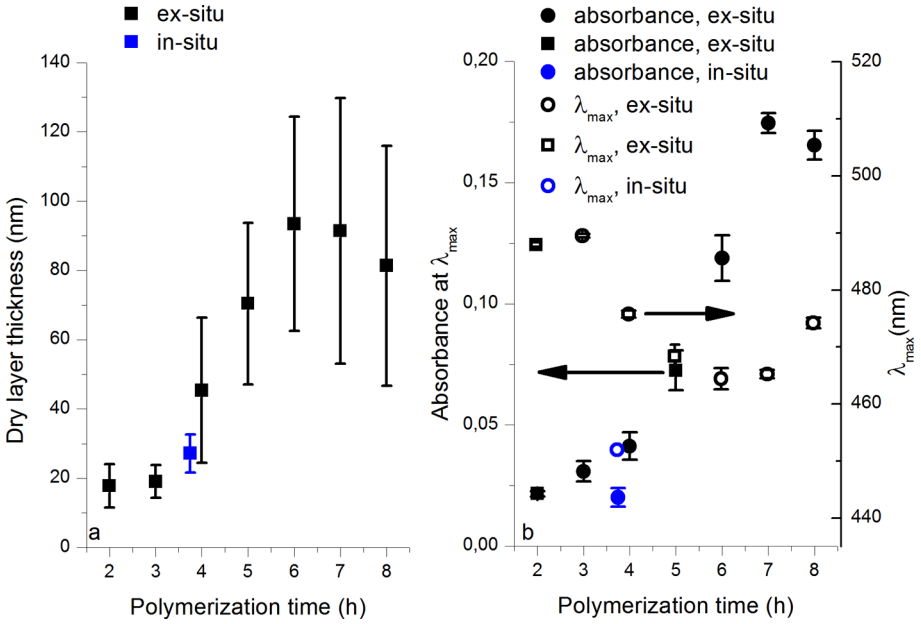

Figure 4. (a, Left) Dry thickness data from AFM measurements and (b, right) wavelength of maximal absorbance and its absorbance from both samples. The single data point from the *in situ* grafted sample results from the final polymer layer that was grafted during the SHG measurements.

polymer and, therefore, shows less NLO signal. In addition, in comparison to the initial stages of the polymerization, the SHG signal shows a faster signal increase from 4 to 7 h of polymerization time. Moreover, a second trend manifests itself in the data, namely, the ratio of the NLO signal from the two incident polarization combinations changes dramatically with polymerization time.

To quantify the changes in the polymer conformation, we deduced the average tilt angle (φ) and distribution width (σ) of the chromophoric side groups from the ratio of the two tensor components that contribute to the SHG signal, $\chi^{(2)}_{zzz}$ and $\chi^{(2)}_{zxx}$ (the indices refer to the laboratory *xyz* axis system, as defined in the middle panel of Figure 1).[12,13,15,38] The values of $\chi^{(2)}_{zzz}$ and $\chi^{(2)}_{zxx}$ were obtained from our polarized SHG data using a fitting procedure, and suiting tilt angle−distribution combinations were obtained by a numerical method that was previously described by Simpson et al.[15,30] The resulting average tilt angle intervals, for the initial and final stages of the polymerization, are depicted in Figure 3a, while the relation between the average tilt angle (φ) and the root-mean-square distribution width σ is plotted in Figure 3b. To maintain a clear and interpretable figure, only a selection of the data is plotted. For the *in situ* grafted sample, data were collected for three positions on the surface, of which the data of only one position is shown in Figure 3b. The data of the remaining two positions can be found in the Supporting Information. The tilt angles (and errors on these values) of all of the measured samples, under the assumption of a narrow tilt angle distribution, are provided in the Supporting Information.

From the data of the *in situ* polymerized sample in Figure 3b, it follows that, assuming narrow distributions of the tilt angles, during the early stages of the polymerization reaction, the chromophoric side groups are angled at least at 75° from the surface normal. A chromophore with an average molecular tilt angle of 75° is a chromophore oriented parallel to a conical region angled 75° from the surface normal. No absolute orientation (up- or downward tilted) of the chromophore is provided by the used methods. From Figure 3b, it follows that even higher average tilt angles are produced in case broader distribution widths are assumed. Such orientation, quasi-parallel to the surface, is often observed with these types of chromophores when they are physisorbed or chemisorbed on glass substrates.[35,36,39,40] If the true average tilt angle distribution remains relatively narrow, the tilt angle follows a steep decrease during the first 3 h and eventually halts at 56.6° ± 0.1°. This angle should not be confused or compared to 57.4°, the magic angle for UV−vis measurements (the magic angle for SHG is 39.2°). During the third polymerization hour, the comparability between both samples is justified by their nearly identical tilt angles. Next to a change in the tilt angle (with a constant narrow distribution of tilt angles), also a broadening of the tilt angle distribution (combined with a constant average tilt angle) or a combination of the two mechanisms could explain our SHG data (see Figure 3b).[13,41,42] In future work, additional methods, such as the null angle method, could be used to further investigate the tilt angle changes with polymerization time.[43,44] In any case, both samples show a comparable trend of the combination of the distribution of tilt angles and average tilt angle. The initial conformation that consists of chromophores aligned relatively flat to the surface changes during the polymerization toward a conformation of a collection of chromophores with a larger tilt angle distribution or a generally decreased tilt angle. A larger tilt angle distribution could potentially arise from a progressively increased disordered polymer film.

In Figure 4, data from (a) AFM and (b) UV−vis measurements of both samples are plotted. The wavelengths of maximal absorbance, absorbance values, and corresponding error bars are determined using a fitting procedure (see the Supporting Information), except for the *ex situ* samples at 2 and 5 h, of which the average values and errors originate from two measurements. The symbols used for the data originating from two measurements are shown in another symbol (■, □). The thickness of the dry polymer layer remains practically unchanged for the first 3 h of polymerization. Then, during the fourth hour of polymerization, the thickness increases

DOI: 10.1021/acs.langmuir.7b00172
Langmuir 2017, 33, 4157−4163

dramatically and, eventually, halts at around 90 nm. With polymerization time, the standard deviation increases. This illustrates that a relatively rough surface is synthesized. In contrast, the absorbance at the maximal wavelength shows a moderate increase during the first 3 h of polymerization and a more intense increase starting from the fifth hour of polymerization. The *ex situ* sample taken at 8 h of polymerization time shows a lower absorbance, which corresponds to a lower monomer content and, therefore, also explains its lower NLO signal intensity. Please note that the *in situ* grafted sample, in contrast to the *ex situ* grafted sample, has only polymer on one side of the substrate, hence, its lower absorbance value. In addition, the wavelength of maximal absorbance shows a blue shift with increased polymerization time, indicating an increasingly less parallel side-by-side alignment of the chromophoric side groups (which can be envisaged as being electric dipoles).[45−48] The blue shift is situated between 3 and 5 h of polymerization time, and with the exception of the sample grafted for 8 h, the decrease of the wavelength of maximal absorbance halts. Intuitively, the less parallel stacking results from interactions of chromophoric side groups from neighboring polymer chains, with their polymer backbones growing parallel in the same direction.[49]

The grafting density σ_{polymer} provides the link between the measured polymer thickness and the length of the polymer; hence, it governs the conformation of the polymeric system and is generally described by

$$\sigma_{\text{polymer}} = \frac{h\rho N_a}{M_n}$$

with h being the thickness of the dry polymer film, ρ being the bulk density of the polymer, N_a being Avogadro's number, and M_n being the number-average molecular weight of the polymer.[50] For example, with the other experimental conditions, such as solvent and temperature, equal, increasing the thickness of the dry polymer layer by adding monomers causes changes in the polymer conformation. For surface-tethered polymers, with the introduction of more monomers to the polymer chain, the polymer changes its conformation from lying flat on the surface with only a negligible thickness increase with polymerization time, i.e., the "pancake" conformation, to a stretched conformation accompanied by a linear thickness increase with polymerization time, i.e., the "brush-type" conformation. Because SHG offers information regarding the tilt angle or its distribution (and, therefore, also the polymer conformation), AFM generates the dry thickness of the polymer layer, and UV−vis gives information on the alignment of the chromophoric side groups and the amount of chromophoric material, the combination of the data from these three techniques offers a method to probe conformational changes in surface-tethered polymers. Our results infer that, after 3 h of polymerization time, a conformational change occurs as a result of the occurrence of changes in the grafting density, caused by crowding effects evidenced by the sudden thickness increase of the dry polymer layer,[10,51] provided that the change in the number-average molecular weight does not overpower the increase in grafting density. The latter situation would also imply an increase in dry film thickness.

The conformational change, during the fourth hour of the synthesis, causes a dramatic increase of the observed dry film thickness, in combination with a halted tilt angle decline or halted tilt angle distribution change and a decrease of the parallel alignment of the electric dipoles of the chromophoric side groups. This suggests that the grafted polymers experience an enhanced crowding effect during the fourth hour of polymerization that drives the polymer chains to grow with their backbone more perpendicularly from the surface, representing a pancake-to-brush transition. This is evidenced by the change from a negligible thickness increase during the initial stages of the polymerization to a linear thickness increase. During the "pancake" stage, the polymer length increases but, instead of creating a thicker polymeric layer by growing away from the surface, the polymer has sufficient room to stay mainly adsorbed on the surface.[52]

Literature reports regarding similar chromophore-modified polymer brushes are focused around polymers with liquid crystal (LC) side groups.[33,37,49,53] Hamelinck et al. observed that the LC side chains of relatively short polymer brushes produce a homeotropic alignment, i.e., parallel to the surface normal, as a result of a coiled conformation of the backbone. Thicker brushes were found to render a decreased homeotropicity, resulting in a tilted alignment of the LC side groups.[37] Uesuka et al. used UV−vis spectroscopy to determine the changes in the order parameter and side-group orientation of a surface-grafted LC polymer with increased polymerization time.[31,49] In contrast to our results, they found a linear relationship between the polymerization time and absorbance increase. They concluded that the reorientation from the side groups of the polymer changes from an initially random orientation toward an orientation parallel to the surface at long polymerization times, where the decreased flexibility of the longer polymer chains aligned the polymers more perpendicular to the surface.[31,49] These literature results indicate that the reached molecular conformations and tilt angles of the side groups depend highly upon the experimental conditions and the used chemical system and change abruptly with chain density. Our data, originating from both a NLO and linear optical technique and AFM, also show dramatic effects on the polymer conformation with increased polymerization time, if the conformation changes of the backbone are reflected in the behavior of the chromophoric side groups. Moreover, the observed trends in polymer layer thickness and polymer conformation are efficiently probed by polarized SHG itself, by monitoring the signal intensity increase or the average molecular tilt angle, respectively. We therefore conclude that polarized SHG is an efficient tool to study these conformational changes and polymer growth *in situ* and *ex situ*.

SUMMARY AND CONCLUSION

We have grafted chromophore-modified polymer brushes from glass substrates and characterized their properties using AFM, UV−vis spectroscopy, and polarized SHG. To the best of our knowledge, we presented the first *in situ* SHG optical measurement of the polymerization of a polymer brush using SI-ARGET ATRP. The results confirm that the presence of very thin tethered polymer layers and the progression of the polymeric growth can be probed *in situ* and *ex situ* using polarized SHG. The average tilt angles of the chromophoric side groups of the grafted polymers as well as their distribution were found to change with polymerization time. A combination of the SHG data with results from AFM and UV−vis enabled us to pinpoint a conformational change that occurred in the fourth polymerization hour. The conformational change is identified as a "pancake-to-brush" transition. Moreover, we conclude that

DOI: 10.1021/acs.langmuir.7b00172
Langmuir 2017, 33, 4157−4163

polarized SHG is an efficient tool to study these conformational changes and polymer growth *in situ* and *ex situ*.

■ ASSOCIATED CONTENT

Supporting Information

The Supporting Information is available free of charge on the ACS Publications website at DOI: 10.1021/acs.langmuir.7b00172.

Detailed synthesis procedure of the samples containing the silanization and polymerization steps, details regarding the synthesis of the modified initiator silane and the chromophore-modified monomer, information regarding the used SHG setup, and additional SHG, UV−vis, and AFM measurements (PDF)

■ AUTHOR INFORMATION

Corresponding Authors

*E-mail: steven.deckers@biw.kuleuven.be.
*E-mail: m.a.vanderveen@tudelft.nl.

ORCID

Steven Deckers: 0000-0003-3389-0348
Guy Koeckelberghs: 0000-0003-1412-8454

Notes

The authors declare no competing financial interest.

■ ACKNOWLEDGMENTS

Christ Glorieux acknowledges Fonds Wetenschappelijk Onderzoek (FWO)—Vlaanderen for financial support (FWO Research Project G.0360.09). The authors acknowledge Dirk De Vos for his helpful contributions. Monique A. van der Veen and Steven Deckers are also grateful to the Onderzoeksfonds KU Leuven/Research Fund KU Leuven for a CREA grant.

■ REFERENCES

(1) Matyjaszewski, K.; Dong, H.; Jakubowski, W.; Pietrasik, J.; Kusumo, A. Grafting from Surfaces for "everyone": ARGET ATRP in the Presence of Air. *Langmuir* **2007**, *23*, 4528−4531.

(2) Huang, X.; Doneski, L. J.; Wirth, M. J. Surface-Confined Living Radical Polymerization for Coatings in Capillary Electrophoresis. *Anal. Chem.* **1998**, *70*, 4023−4029.

(3) Huang, X.; Wirth, M. J. Surface-Initiated Radical Polymerization on Porous Silica. *Anal. Chem.* **1997**, *69*, 4577−4580.

(4) Ejaz, M.; Yamamoto, S.; Ohno, K.; Tsujii, Y.; Fukuda, T. Controlled Graft Polymerisation of Methyl Methacrylate on Silicon Substrate by the Combined Used of the Langmuir−Blodgett and Atom Transfer Radical Polymerization Techniques. *Macromolecules* **1998**, *31*, 5934−5936.

(5) Min, K.; Gao, H.; Matyjaszewski, K. Use of Ascorbic Acid as Reducing Agent for Synthesis of Well-Defined Polymers by ARGET ATRP. *Macromolecules* **2007**, *40*, 1789−1791.

(6) Mastan, E.; Xi, L.; Zhu, S. What Limits the Chain Growth from Flat Surfaces in Surface-Initiated ATRP: Propagation, Termination or Both? *Macromol. Theory Simul.* **2015**, *24*, 89−99.

(7) Barbey, R.; Lavanant, L.; Paripovic, D.; Schüwer, N.; Sugnaux, C.; Tugulu, S.; Klok, H.-A. Polymer Brushes via Surface-Initiated Controlled Radical Polymerization: Synthesis, Characterization, Properties, and Applications. *Chem. Rev.* **2009**, *109*, 5437−5527.

(8) Feng, W.; Brash, J.; Zhu, S. Atom-Transfer Radical Grafting Polymerization of 2-Methacryloyloxyethyl Phosphorylcholine from Silicon Wafer Surfaces. *J. Polym. Sci., Part A: Polym. Chem.* **2004**, *42*, 2931−2942.

(9) Brittain, W. J.; Minko, S. A Structural Definition of Polymer Brushes. *J. Polym. Sci., Part A: Polym. Chem.* **2007**, *45*, 3505−3512.

(10) Chen, J. K.; Hsieh, C. Y.; Huang, C. F.; Li, P. min. Characterization of Patterned Poly(methyl Methacrylate) Brushes under Various Structures upon Solvent Immersion. *J. Colloid Interface Sci.* **2009**, *338*, 428−434.

(11) Ishida, N.; Biggs, S. Salt-Induced Structural Behavior for poly(N-Isopropylacryamide) Grafted onto Solid Surface Observed Directly by AFM and QCM-D. *Macromolecules* **2007**, *40*, 9045−9052.

(12) Heinz, T.; Tom, H.; Shen, Y. Determination of Molecular Orientation of Monolayer Adsorbates by Optical Second-Harmonic Generation. *Phys. Rev. A: At., Mol., Opt. Phys.* **1983**, *28*, 1883−1885.

(13) Simpson, G. J.; Rowlen, K. L. An SHG Magic Angle: Dependence of Second Harmonic Generation Orientation Measurements on the Width of the Orientation Distribution. *J. Am. Chem. Soc.* **1999**, *121*, 2635−2636.

(14) Zhang, W.; Wang, H.; Zheng, D. Quantitative Measurement and Interpretation of Optical Second Harmonic Generation from Molecular Interfaces. *Phys. Chem. Chem. Phys.* **2006**, *8*, 4041−4052.

(15) van der Veen, M. a; Valev, V. K.; Verbiest, T.; De Vos, D. E. In Situ Orientation-Sensitive Observation of Molecular Adsorption on a Liquid/zeolite Interface by Second-Harmonic Generation. *Langmuir* **2009**, *25*, 4256−4261.

(16) van der Veen, M. A.; de Roeck, M.; Vankelecom, I. F. J.; de Vos, D. E.; Verbiest, Z. The Use of Second-Harmonic Generation to Study Diffusion through Films under a Liquid Phase. *ChemPhysChem* **2010**, *11*, 870−874.

(17) Leng, C.; Han, X.; Shao, Q.; Zhu, Y.; Li, Y.; Jiang, S.; Chen, Z. In Situ Probing of the Surface Hydration of Zwitterionic Polymer Brushes: Structural and Environmental Effects. *J. Phys. Chem. C* **2014**, *118*, 15840−15845.

(18) Schürer, B.; Hoffmann, M.; Wunderlich, S.; Harnau, L.; Peschel, U.; Ballauff, M.; Peukert, W. Second Harmonic Light Scattering from Spherical Polyelectrolyte Brushes. *J. Phys. Chem. C* **2011**, *115*, 18302−18309.

(19) Zhang, X.; Wang, P.; Zhu, P.; Ye, C.; Xi, F. Second Order Non-Linear Optical Materials Based on Poly(p-Chloromethyl Styrene). *Macromol. Chem. Phys.* **2000**, *201*, 1853−1857.

(20) Zhang, Z.; Chao, T.; Chen, S.; Jiang, S. Superlow Fouling Sulfobetaine and Carboxybetaine Polymers on Glass Slides. *Langmuir* **2006**, *22*, 10072−10077.

(21) Zhang, Z.; Vaisocherová, H.; Cheng, G.; Yang, W.; Xue, H.; Jiang, S. Nonfouling Behavior of Polycarboxybetaine-Grafted Surfaces: Structural and Environmental Effects. *Biomacromolecules* **2008**, *9*, 2686−2692.

(22) Wang, J. S.; Matyjaszewski, K. Controlled/"living" radical Polymerization. Atom Transfer Radical Polymerization in the Presence of Transition-Metal Complexes. *J. Am. Chem. Soc.* **1995**, *117*, 5614−5615.

(23) Braunecker, W. A.; Pintauer, T.; Tsarevsky, N. V.; Kickelbick, G.; Matyjaszewski, K. Towards Understanding Monomer Coordination in Atom Transfer Radical Polymerization: Synthesis of [CuI(PMDETA)(π-M)][BPh_4] (M = Methyl Acrylate, Styrene, 1-Octene, and Methyl Methacrylate) and Structural Studies by FT-IR and ^{1}H NMR Spectroscopy and X-Ray. *J. Organomet. Chem.* **2005**, *690*, 916−924.

(24) Braunecker, W. A.; Tsarevsky, N. V.; Pintauer, T.; Gil, R. R.; Matyjaszewski, K. Quantifying Vinyl Monomer Coordination to Cu I in Solution and the Effect of Coordination on Monomer Reactivity in Radical Copolymerization. *Macromolecules* **2005**, *38*, 4081−4088.

(25) Wen, Y. C.; Zha, S.; Liu, X.; Yang, S.; Guo, P.; Shi, G.; Fang, H.; Shen, Y. R.; Tian, C. Unveiling Microscopic Structures of Charged Water Interfaces by Surface-Specific Vibrational Spectroscopy. *Phys. Rev. Lett.* **2016**, *116*, 1−5.

(26) Ohno, P. E.; Saslow, S. A.; Wang, H.; Geiger, F. M.; Eisenthal, K. B. Phase-Referenced Nonlinear Spectroscopy of the α-Quartz/water Interface. *Nat. Commun.* **2016**, *7*, 13587.

(27) Geiger, F. M. Second Harmonic Generation, Sum Frequency Generation, and χ (3): Dissecting Environmental Interfaces with a Nonlinear Optical Swiss Army Knife. *Annu. Rev. Phys. Chem.* **2009**, *60*, 61−83.

DOI: 10.1021/acs.langmuir.7b00172
Langmuir 2017, 33, 4157−4163

(28) Verbiest, T.; Clays, K.; Rodriguez, V. *Second-Order Nonlinear Optical Characterization Techniques*; CRC Press: Boca Raton, FL, 2009.
(29) Flörsheimer, M.; Bösch, M.; Brillert, C.; Wierschem, M.; Fuchs, H. Second-Harmonic Imaging of Surface Order and Symmetry. *Thin Solid Films* **1998**, *327*−*329*, 241−246.
(30) Zhuang, X.; Miranda, P.; Kim, D.; Shen, Y. Mapping Molecular Orientation and Conformation at Interfaces by Surface Nonlinear Optics. *Phys. Rev. B: Condens. Matter Mater. Phys.* **1999**, *59*, 12632−12640.
(31) Uekusa, T.; Nagano, S.; Seki, T. Highly Ordered In-Plane Photoalignment Attained by the Brush Architecture of Liquid Crystalline Azobenzene Polymer. *Macromolecules* **2009**, *42*, 312−318.
(32) S'Heeren, G.; Derhaeg, L.; Verbiest, T.; Samyn, C.; Persoons, A. Nonlinear Optical Properties of Polymers and Thin Polymer Films. *Makromol. Chem., Macromol. Symp.* **1993**, *69*, 193−203.
(33) Peng, B.; Johannsmann, D.; Rühe, J. Polymer Brushes with Liquid Crystalline Side Chains. *Macromolecules* **1999**, *32*, 6759−6766.
(34) Li, D.; Ratner, M. A.; Marks, T. J.; Zhang, C.; Yang, J.; Wong, G. K. Chromophoric Self-Assembled Multilayers. Organic Superlattice Approaches to Thin-Film Nonlinear Optical Materials. *J. Am. Chem. Soc.* **1990**, *112*, 7389−7390.
(35) Verbiest, T.; Samyn, C.; Persoons, A. Second-Harmonic Generation from Floating Langmuir Layers of an Azobenzene-Functionalized Copolymer. *Thin Solid Films* **1994**, *242*, 139−141.
(36) Deckers, S.; Van Steerteghem, N.; Glorieux, C.; Verbiest, T.; van der Veen, M. A. Acoustic Effects on Nonlinear Optical Processes. *Proceedings of the SPIE Organic Photonics + Electronics*; San Diego, CA, Aug 28−Sept 1, 2016; 99390F, DOI: 10.1117/12.2236958.
(37) Hamelinck, P. J.; Huck, W. T. S. Homeotropic Alignment on Surface-Initiated Liquid Crystalline Polymer Brushes. *J. Mater. Chem.* **2005**, *15*, 381.
(38) Heinz, T.; Chen, C.; Ricard, D.; Shen, Y. Spectroscopy of Molecular Monolayers by Resonant Second-Harmonic Generation. *Phys. Rev. Lett.* **1982**, *48*, 478−481.
(39) Zhang, T. G.; Zhang, C. H.; Wong, G. K. Determination of Molecular Orientation in Molecular Monolayers by Second-Harmonic Generation. *J. Opt. Soc. Am. B* **1990**, *7*, 902.
(40) He, G.; Xu, Z. Tuning the Orientation of Molecules at Solid−Liquid Interfaces Using an Electrochemical Potential. *J. Phys. Chem. B* **1997**, *101*, 2101−2104.
(41) Ekhoff, J. A.; Westerbuhr, S. G.; Rowlen, K. L. Evidence of Spontaneous Multilayer Formation for Disperse Red-1 at a Fused-silica/2-Propanol Interface. *Langmuir* **2001**, *17*, 7079−7084.
(42) Simpson, G.; Westerbuhr, S.; Rowlen, K. Molecular Orientation and Angular Distribution Probed by Angle-Resolved Absorbance and Second Harmonic Generation. *Anal. Chem.* **2000**, *72*, 887−898.
(43) Achtyl, J. L.; Buchbinder, A. M.; Geiger, F. M. Hydrocarbon on Carbon: Coherent Vibrational Spectroscopy of Toluene on Graphite. *J. Phys. Chem. Lett.* **2012**, *3*, 280−282.
(44) Stokes, G. Y.; Buchbinder, A. M.; Gibbs-Davis, J. M.; Scheidt, K. A.; Geiger, F. M. Chemically Diverse Environmental Interfaces and Their Reactions with Ozone Studied by Sum Frequency Generation. *Vib. Spectrosc.* **2009**, *50*, 86−98.
(45) Hirano, Y.; Tokuoka, Y.; Kawashima, N.; Ozaki, Y. Origin of Formation of Blue-Shifted Aggregates Including H-Aggregates in Mixed Langmuir-Blodgett Films of Merocyanine Dye Investigated by Polarized Visible and Infrared Spectroscopy. *Vib. Spectrosc.* **2007**, *43*, 86−96.
(46) Ding, L.; Russell, T. P. A Photoactive Polymer with Azobenzene Chromophore in the Side Chains. *Macromolecules* **2007**, *40*, 2267−2270.
(47) Buffeteau, T.; Lagugné Labarthet, F.; Pézolet, M.; Sourisseau, C. Photoinduced Orientation of Azobenzene Chromophores in Amorphous Polymers as Studied by Real-Time Visible and FTIR Spectroscopies. *Macromolecules* **1998**, *31*, 7312−7320.
(48) Brown, D.; Natansohn, a.; Rochon, P. Azo Polymers for Reversible Optical Storage. 5. Orientation and Dipolar Interactions of Azobenzene Side Groups in Copolymers and Blends Containing Methyl Methacrylate Structural Units. *Macromolecules* **1995**, *28*, 6116−6123.
(49) Uekusa, T.; Nagano, S.; Seki, T. Unique Molecular Orientation in a Smectic Liquid Crystalline Polymer Film Attained by Surface-Initiated Graft Polymerization. *Langmuir* **2007**, *23*, 4642−4645.
(50) Laurent, P.; Souharce, G.; Duchet-Rumeau, J.; Portinha, D.; Charlot, A. Pancake"vs. Brush-like Regime of Quaternizable Polymer Grafts: An Efficient Tool for Nano-Templating Polyelectrolyte Self-Assembly. *Soft Matter* **2012**, *8*, 715−725.
(51) de Gennes, P. G. Conformations of Polymers Attached to an Interface. *Macromolecules* **1980**, *13*, 1069−1075.
(52) Wu, T.; Efimenko, K.; Genzer, J. Combinatorial Study of the Mushroom-to-Brush Crossover in Surface Anchored Polyacrylamide. *J. Am. Chem. Soc.* **2002**, *124*, 9394−9395.
(53) Peng, B.; Rühe, J.; Johannsmann, D. Homogeneously Aligned Liquid-Crystal Polymer Brushes. *Adv. Mater.* **2000**, *12*, 821−824.

DOI: 10.1021/acs.langmuir.7b00172
Langmuir 2017, 33, 4157−4163